Optics Letters

Real-time random grating sensor array for quasi-distributed sensing based on wavelength-to-time mapping and time-division multiplexing

Jingxuan Liu,[1,2] Ping Lu,[3] Stephen J. Mihailov,[3] Muguang Wang,[2] and Jianping Yao[1,*]

[1]Microwave Photonics Research Laboratory, School of Electrical Engineering and Computer Science, University of Ottawa, Ontario K1N 6N5, Canada
[2]Key Laboratory of All Optical Network and Advanced Telecommunication Network, Ministry of Education, Institute of Lightwave Technology, Beijing Jiaotong University, Beijing 100044, China
[3]National Research Council Canada, Ottawa, Ontario K1A 0R6, Canada
*Corresponding author: jpyao@eecs.uottawa.ca

Received 6 November 2018; revised 7 December 2018; accepted 11 December 2018; posted 12 December 2018 (Doc. ID 351168); published 11 January 2019

A real-time random grating sensor array for quasi-distributed sensing based on spectral-shaping and wavelength-to-time (SS-WTT) mapping and time-division multiplexing is proposed and experimentally demonstrated. The sensor array consists of multiple random gratings written in a single-mode fiber (SMF) at different physical locations. When the temperature or strain applied to a particular random grating is changed, the central wavelength of the reflection spectrum of the random grating will change, which is converted to the time domain as a time shift based on SS-WTT using a linearly chirped fiber Bragg grating. After detection at a photodetector, an electrical waveform with the time shift information encoded in the random waveform is obtained, which is further compressed by correlation to increase the time resolution. As a demonstration, a real-time quasi-distributed sensing system based on a two-random-grating array is implemented. The results show that the sensing resolutions for temperature and strain are 0.23°C and 2.5 με, respectively, and the accuracies for temperature and strain are 0.11°C and 1.2 με, respectively. Compared with a conventional quasi-distributed sensor, our proposed sensing system has key advantages, including real-time sensing, high-resolution interrogation, and large scalability.

https://doi.org/10.1364/OL.44.000379

Optical fiber sensors based on fiber Bragg gratings (FBGs) have drawn a great deal of attention due to distinctive advantages such as small size, low cost, anti-erosion ability, immunization to electromagnetic interference, and multiplexing capability. In many applications where multiple sensing points are demanded such as building structure monitoring, a series of FBGs is distributed to the sensing area to achieve quasi-distributed sensing. Wavelength-division multiplexing (WDM) [1,2] and time-division multiplexing (TDM) [3,4] are two common methods for quasi-distributed sensing. In the case of WDM, the capacity is limited by the ratio between the spectral range of a broadband light source and the wavelength width assigned to every FBG which is linked to the maximum number of distributed sensors that can be accommodated [5,6]. For TDM, reflected pulses with different time delays from different FBGs can distinguish their positions which would greatly reduce the spectral range requirement compared to a quasi-distributed sensor based on WDM. By using an ultraweak FBG array, the crosstalk from other FBGs is at least 10 dB weaker than that of the reflected signal which is small and can be negligible. The number of FBGs can be over 1000 [7]. However, for both WDM and TDM, the sensing information is encoded in the Bragg wavelengths of the FBGs, and the interrogation should be done by scanning the entire spectral range using an optical spectrum analyzer (OSA) [8]. Due to the relatively low speed of an OSA, the interrogation speed is limited which cannot meet the requirements for applications such as chemical and biological reaction detection where high-speed interrogation is needed [9]. In addition, the full width at half-maximum of an FBG is relatively wide, which would limit the sensing resolution and accuracy.

Microwave photonics which combines the optical and microwave engineering gives an effective solution to realize high-speed and high-resolution interrogation. In Ref. [10], a high-resolution strain sensor based on chirped microwave pulse compression was proposed and demonstrated. A chirped microwave waveform with the sensing information encoded as the center frequency change of the waveform was generated based on spectral shaping and wavelength-to-time (SS-WTT) mapping. By detecting the peak location of the compressed microwave waveform, high-resolution interrogation was achieved. However, the chirped microwave waveform was generated based on SS-WTT mapping in which the spectral shaping was done using a fiber-based Mach–Zehnder interferometer which is ultra-unstable. In addition, the technique is difficult to expand to cover multiple sensing points for quasi-distributed sensing.

Recently, random fiber gratings have been employed for high-resolution sensing. A random fiber grating can be fabricated without using a phase mask. In addition, the random spectrum can be significantly compressed to increase the resolution. When the environmental parameters change, a wavelength shift of random reflection spectrum occurs that is similar to the central wavelength shift of a regular FBG. After correlation with the reference spectrum, the random reflection spectrum can be significantly compressed which gives an access to achieve high-resolution sensing [11]. However, to measure the spectrum, an OSA is needed, making the interrogation speed slow.

In this Letter, we propose and demonstrate a quasi-distributed sensing system using a random grating sensor array to achieve real-time and high-resolution sensing based on SS-WTT mapping. The sensor array consists of multiple random gratings written in a single-mode fiber (SMF) at different physical locations. The wavelength shifts of the random gratings in the optical domain are converted to time shifts in the electrical domain based on SS-WTT mapping. In the proposed system, an ultrashort pulse from a mode-locked laser (MLL) source is sent to the random grating array. To achieve effective quasi-distributed sensing, the random gratings are made to have weak reflectivity to ensure that the ultrashort pulse can reach the grating at the other end of the grating array. Since different random gratings have different, but unique, reflection spectra located at different locations, a series of reflected waveforms with different spectrally shaped spectra and different time delays is generated. By passing the waveforms through a linearly chirped fiber Bragg grating (LCFBG) to perform WTT mapping and detecting them at a photodetector (PD), electrical random waveforms with temporal shapes identical to the shapes of the spectrally shaped spectra are obtained. By pulse compression, the temporal waveforms are significantly compressed, making the interrogation resolution significantly increased. Since the temporal locations reflect the wavelength shifts of the random gratings, by measuring the time shifts, the sensing information is obtained.

Figure 1 shows the configuration of the proposed real-time quasi-distributed sensing system. An ultrashort pulse generated by a MLL source is sent to a tunable optical filter (OF) to control the spectral width, and then sent to a random grating array. The spectrum of the ultrashort pulse is then spectrally shaped by the random gratings to generate a series of pulses with different time delays. The spectrum-shaped pulses are transmitted to an LCFBG serving as a dispersive element to achieve WTT mapping. After amplified by an erbium-doped fiber amplifier

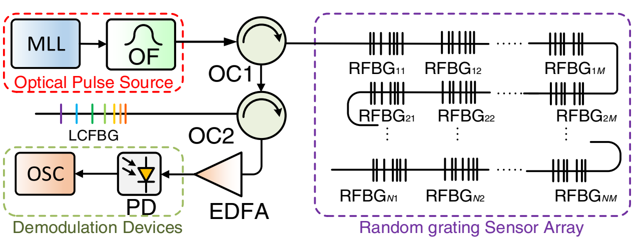

Fig. 1. Schematic diagram of the proposed real-time sensing system. MLL, mode-locked laser; OF, optical filter; LCFBG, linearly chirped fiber Bragg grating; EDFA, erbium-doped fiber amplifier; PD, photodetector; OSC, oscilloscope.

(EDFA), the mapped optical pulses are detected at a PD. Electrical random waveforms that have the same shapes as those of the reflected spectra are generated with the temporal shifts corresponding to the wavelength shifts. To increase the interrogating resolution, the electrical random waveforms are compressed. The wavelength shifts of the random gratings are translated to the time shifts of the compressed pulses. Since the random pulses are significantly compressed, the sensing resolution is significantly increased.

For the proposed distributed sensor, the key device is the random grating sensor array. As shown in Fig. 1, the sensor array has N rows of series connected random gratings with each row having M random gratings. The time delay between the two pulses reflected by two adjacent gratings is given by

$$T_{i-1,i} = \frac{2nL_{i-1,i}}{c}, \tag{1}$$

where $T_{i-1,i}$ is the time taken to traverse twice the distance between the $(i-1)$th and ith random gratings, n is the refractive index of the fiber core, $L_{i-1,i}$ is the distance between two adjacent random gratings, and c is the velocity of light in vacuum.

It is different from a regular FBG which is inscribed by exposing a photosensitive fiber under a periodic fringe pattern of a UV light, where a phase mask is used to produce the periodic fringe pattern under which the refractive index of a fiber is changed. A random grating is fabricated by using a femtosecond laser to modify the refractive index of the fiber core spot by spot with random variations of the spot spacing. The superimposition of the multiple core-core mode coupling and the core-cladding mode coupling leads to an irregular reflection spectrum of the random grating. The intensity of the reflected light from all spots could be expressed as [11]

$$\begin{aligned} I_R \approx P_0 \Bigg\{ & \sum_{k=1}^{W}\sum_{j=1}^{W} \exp[-\alpha(L_k + L_j)] r_k^{\mathrm{core}} r_j^{\mathrm{core}} \\ & \times \exp[i(\varphi_k^{\mathrm{core}} - \varphi_j^{\mathrm{core}})] + 2a \sum_{k=1}^{W}\sum_{j=1}^{W} \\ & \times \exp[-\alpha(L_k + L_j)] r_k^{\mathrm{core}} r_j^{\mathrm{clad}} \exp[i(\varphi_k^{\mathrm{core}} - \varphi_j^{\mathrm{clad}})] \Bigg\} = P_0 R, \end{aligned} \tag{2}$$

where P_0 is the input power of the pulse; W is the total number of the spots in the random grating; α is the averaged attenuation of the unit-length random grating; L_k and L_j are the fiber length at the kth and jth spot; r_k^{core}, r_j^{core}, r_k^{clad}, and r_j^{clad} are the reflectivity of the core mode and cladding mode at the kth and jth spot; $\varphi_k^{\mathrm{core}}$, $\varphi_j^{\mathrm{core}}$, $\varphi_k^{\mathrm{clad}}$, and $\varphi_j^{\mathrm{clad}}$ are the phase of the core and claddings modes at the kth and jth spot; a is the back coupling coefficient of the cladding modes; and R is the reflectivity of the random grating. In this case, due to the weak intensity of the cladding modes, the interferences between the cladding modes have been neglected. The reflectivity of the random grating is relatively low which is the essential condition in a sensor array to ensure sufficient transmitted power and low crosstalk between adjacent random gratings. Thus, in the random grating sensor array, the reflected power from the pth random grating is given by

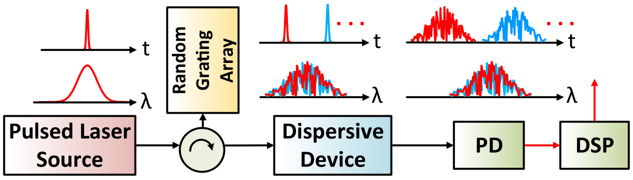

Fig. 2. Principle of wavelength-to-time mapping in the real-time sensing system based on the random grating sensor array.

$$P_p = P_0 \times R_p \times \prod_{q=1}^{p-1} (1 - R_q)^2, \quad (3)$$

where R_p and R_q are the reflectivity of the pth and qth random gratings in the random grating sensor array ($q < p$).

Since different random gratings have different reflected spectra located at different physical locations, the pulse is reflected by the random gratings in sequence to form a series of pulses with different time delays and different shaped spectra. Since the spectra of the random gratings are very broad, the reflected spectra are overlapped, as shown in Fig. 2. It is impossible to monitor the wavelength shift of an individual random grating without compressing the spectrum. In addition, the compression of the spectrum will make the interrogation speed low. To solve the problem, we map the spectrum to the time domain, which is done by using an LCFBG. After the WTT mapping, electrical random waveforms having the shaped reflection spectra of the random gratings in the grating array are separated in the time domain. Thus, the wavelength changes of the random gratings in the optical domain due to environmental variations are converted to time shifts in the electrical domain, making real-time sensing possible. In addition, by pulse compression, the electrical waveforms are significantly compressed, making the interrogation resolution significantly increased.

The key strategy of the approach is to convert the random spectrum of a shaped pulse to the time domain with the shape of the temporal waveform identical to the spectrum of the short pulse [12]. When external disturbances such as temperature or strain are applied to a random grating, the interferential lengths and effective refractive indices of the core mode and cladding modes will change which will result in a phase shift corresponding to a spectral shift in the reflection spectrum of the random grating. After SS-WTT mapping, the wavelength shift of the random grating can be translated to the time shift of the electrical random waveform to realize real-time interrogation.

However, the spectrum of the electrical waveform is random and broad, making it difficult to detect the wavelength shift. Thus, a pulse compression based on correlation is employed to extract the spectral shift information. The static temporal waveform is used as a reference. The electrical waveform with a time shift is correlated with the reference. Since they have an identical shape, the pulse is significantly compressed. A peak will emerge in the compressed pulse deviating from the peak location in the auto-correlation spectrum of the reference signal. The temporal location change of the electrical waveform corresponding to the wavelength shift of the reflection spectrum of the random grating is converted to the time shift of the compressed peak.

To prove the concept, a random grating array consisting of two random gratings written in an SMF is fabricated and used as a quasi-distributed sensor. The spacing between the two gratings is 1.32 m, corresponding to a time separation of 12.7 ns. An ultrashort pulse generated by a tunable MLL (PriTel FFL-1550-20) with a pulse width of less than 600 fs is sent to a programmable bandpass optical filter (Waveshaper 4000S) which is tuned at a central wavelength of 1551 nm and a spectral width of 4 nm. Two ultrashort pulses are reflected by the two cascaded random gratings and sent to a LCFBG for WTT mapping. The LCFBG has a dispersion coefficient of 2500 ps/nm. The optical signal at the output of the LCFBG is fed into a 10 GHz PD (Newport) to generate an electrical waveform. The electrical waveform is monitored by a real-time oscilloscope (OSC, Keysight, DSOZ504A). Figure 3(a) shows the optical spectrum at the output of the random grating array in a wavelength range from 1542 to 1557 nm. As can be seen, the spectra of the pulses from the two random gratings are overlapped which makes it difficult to monitor the wavelength shifts. In the time domain, the two electrical random pulses from the two random gratings are separated, as shown in Fig. 3(b). Each of the two pulses has a width of around 10 ns, and the time separation between the two pulses is 12.7 ns. The power of the second electrical random waveform is lower than that of the first one because of the transmission loss of the first grating and the lower reflectivity of the second grating. By reducing the reflectivity of the first random grating and increasing the reflectivity of the second grating, the output power of two electrical random waveforms can be balanced. After pulse compression, the first and second electrical random waveforms are significantly compressed, as shown in Figs. 3(c) and 3(d).

Then a temperature sensing experiment is performed. The reference signal is the electrical random waveform at a temperature of 35°C. When the temperature increases, the reflection spectrum of the random grating exhibits a redshift corresponding to a time shift of the electrical random waveform after WTT mapping. By pulse compression, a significantly compressed pulse is produced. The temperature change can be

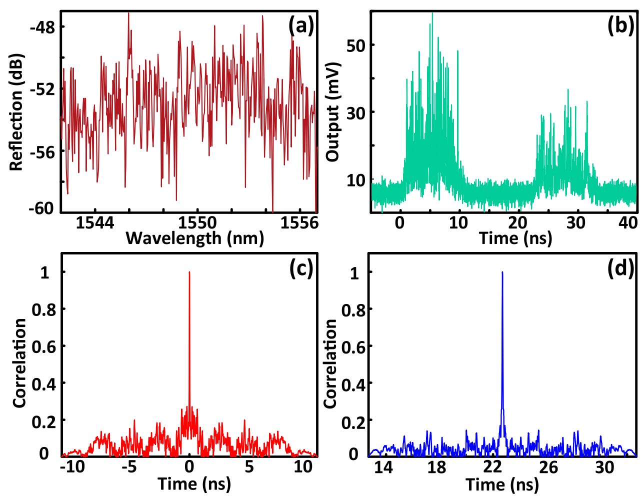

Fig. 3. Spectrum of the (a) reflection spectrum of the random grating array. (b) Two electrical random waveforms. Compressed pulses from two electrical random waveforms of (c) the first and (d) second random grating under static condition.

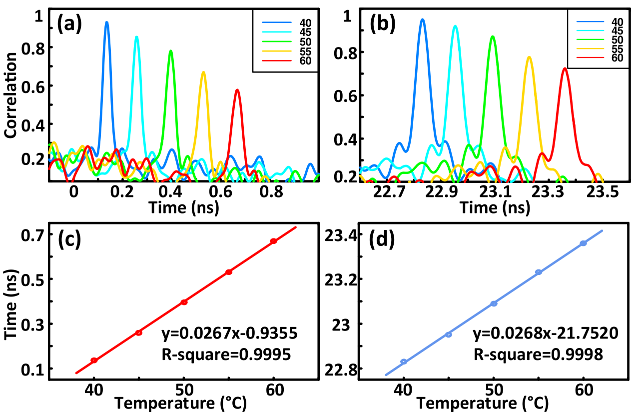

Fig. 4. Compressed pulses for two electrical random pulses from (a) the first and (b) second random gratings under different temperature values. The relationship between the temperature and time shifts of compressed pulses from the (c) first and (d) second electrical random pulses.

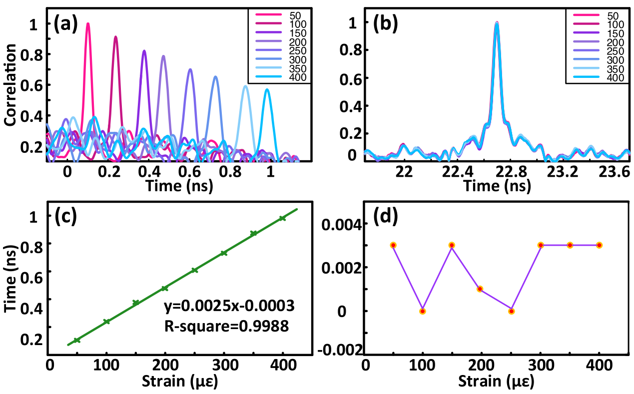

Fig. 5. Compressed pulses from two electrical random pulses of (a) the one with an increased strain and (b) the one with no strain change. (c) Relationship between the strain and time shift of the compressed pulse from the random grating with an increased strain. (d) Stability of the system.

detected by monitoring the time shift of the compressed pulse. Thus, the sensing resolution is improved. If the same temperature is applied to the two random gratings, as can be seen in Figs. 4(a) and 4(b), both of the compressed pulses have an identical time shift. Figures 4(c) and 4(d) show the relationship between the temperature and time shift of the compressed pulses by linear data fitting. The temperature sensitivities of two random gratings are calculated to be 0.0267 and 0.0268 ns/°C. The correlation coefficients (R-squares) are as large as 0.9995 and 0.9998, indicating linear relationship between the time shift and the temperature change.

A strain sensing experiment is performed. In the experiment, the temperature is controlled constant, and a strain is applied to one random grating. Figures 5(a) and 5(b) show the compressed pulses from the two random gratings. The time shift of the compressed pulse from the random grating is increasing when an increased strain is applied. Figure 5(c) shows the relationship between the strain and time shift of the compressed pulse from the random grating with a linear increased strain. Linear data fitting is also shown. The strain sensitivity is calculated to be 0.0025 ns/με with an R-square of 0.9988. Figure 5(d) shows the time locations of the compressed pulse from the random grating with no strain applied. The measurements show that the pulse location is drifting between 0 and 0.003 ns, which is small and indicates good stability of the proposed quasi-distributed sensing system. Thus, the measurement accuracies for temperature and strain are obtained, which are as high as 0.11°C and 1.2 με. In this demonstration, the wavelength changes of the random gratings are converted to time shifts of the compressed peaks which can be accurately measured by a DSP. The resolution of the proposed quasi-distributed sensing system is limited by the sampling rate of the OSC. The sampling rate of the OSC used to collect sensing data is 160 GSa/s, corresponding to a time resolution of 6.25 ps. Thus, the temperature and strain measurement resolutions are 0.23°C and 2.5 με, respectively. In addition, the interrogation speed is 20 MHz which is determined by the repetition rate of the MLL considering that the DSP can operate at an ultrahigh processing speed.

In conclusion, we have proposed and demonstrated a random grating sensor array for real-time quasi-distributed sensing based on SS-WTT mapping. The key to achieving the real-time sensing was to translate the wavelength shifts of the random gratings in the optical domain to temporal location changes in the time domain based on WTT mapping. The high resolution was achieved by pulse compression thanks to the use of random gratings to generate random waveforms which could be highly compressed. A real-time and high-resolution quasi-distributed sensing system was demonstrated. The results showed that the temperature and strain resolutions of the sensor were 0.23°C and 2.5 με, respectively, and the temperature and strain accuracies were 0.11°C and 1.2 με, respectively.

Funding. Natural Sciences and Engineering Research Council of Canada (NSERC).

REFERENCES

1. A. D. Kersey, T. A. Berkoff, and W. W. Morey, Opt. Lett. **18**, 1370 (1993).
2. K. P. Koo and A. D. Kersey, J. Lightwave Technol. **13**, 1243 (1995).
3. R. S. Weis, A. D. Kersey, and T. A. Berkoff, IEEE Photonics Technol. Lett. **6**, 1469 (1994).
4. Y. Wang, J. Gong, D. Y. Wang, B. Dong, W. Bi, and A. Wang, IEEE Photonics Technol. Lett. **23**, 70 (2011).
5. W. Jin, Proc. SPIE **3897**, 468 (1999).
6. C. Hu, H. Wen, and W. Bai, J. Lightwave Technol. **32**, 1406 (2014).
7. Y. Wang, J. Gong, B. Dong, D. Y. Wang, T. J. Shillig, and A. Wang, J. Lightwave Technol. **30**, 2751 (2012).
8. J. Yao, Fiber Integr. Opt. **34**, 204 (2015).
9. F. Patolsky, G. Zheng, and C. M. Lieber, Nat. Protoc. **1**, 1711 (2006).
10. W. Liu, M. Li, C. Wang, and J. Yao, J. Lightwave Technol. **29**, 1239 (2011).
11. Y. Xu, M. Zhang, P. Lu, S. Mihailov, and X. Bao, AIP Adv. **6**, 095009 (2016).
12. J. Yao, Opt. Commun. **284**, 3723 (2011).